Can the Fisher-Lande Process Account for Birds of Paradise and Other Sexual Radiations?

Stevan J. Arnold* **and Lynne D. Houck†**

Department of Integrative Biology, Oregon State University, Corvallis, Oregon 97331

Submitted June 20, 2015; Accepted January 29, 2016; Electronically published April 19, 2016

Online enhancements: appendix. *Dryad data:* http://dx.doi.org/10.5061/dryad.66ft5.2.

ABSTRACT: Models of the Fisher-Lande process (FLP) have been used successfully to explore many aspects of evolution by sexual selection. Despite this success, quantitative tests of these models using data from sexual radiations are rare. Consequently, we do not know whether realistic versions of the FLP can account for the extent and the rate of evolution of sexually selected traits. To answer this question, we generalize the basic FLP model of sexual coevolution and compare predictions of that basic model with patterns observed in an iconic sexual radiation, birds of paradise. Our model tracks the coevolution of male and female traits (two in each sex) while relaxing some restrictive assumptions. Using computer simulations, we evaluate the behavior of the model and confirm that it is an Ornstein-Uhlenbeck (OU) process. We also assess the ability of the FLP to account for the quantitative aspects of ornament evolution in the genus *Paradisaea* using published measurements of display traits and a phylogeny of the genus. Finally, we use the program OUwie to compare model fits to generic OU and Brownian motion processes and to estimate FLP parameters. We show that to explain the sexual radiation of the genus *Paradisaea* one must either invoke extremely weak stabilizing selection on female mating preferences or allow the preference optimum to undergo Brownian motion at a modest rate.

Keywords: phenotypic tango, adaptive radiation, Brownian motion, Ornstein-Uhlenbeck (OU) process, sexual coevolution.

Introduction

Quantitative genetic models for evolution by sexual selection have proliferated even though tests with data have been neglected. This neglect is surprising, since quantitative genetic models of phenotypic models, unlike population genetic models, have enormous potential for evaluation in natural populations (Mead and Arnold 2004). The three dozen or so elaborations of Lande's (1981) quantitative genetic model have included male and female genetic quality in addition to ornaments and preferences, such that a large array of processes have been modeled (e.g., sexy son, good genes, good parents, sexual conflict; Mead and Arnold 2004; Kuijper et al. 2012). Considering just the combinations that result from parameters with two states, more than 250,000 models are now under discussion in the literature. Instead of tackling the enormous task of testing this huge diversity of models, we focus on the basic model that is at the core of the model diversity and outline an approach for testing that basic model—as well as its extensions—with data from sexual radiations. Our approach in testing this basic model could be applied to any of the more elaborate models that have been derived from it.

According to the basic model, sketched by Fisher (1915, [1930] 1958) and specified by Lande (1981), a sexually selected male trait coevolves with female preference for that trait. In the basic model, the female mate choice confers no direct benefits and incurs no costs. The model results in a coevolutionary process that has unstable (runaway) or stable (walk-toward) outcomes. This duality of outcomes also occurs in virtually all of the models based on Lande's (1981) model (Mead and Arnold 2004). Given this duality, it is problematic to refer to the process as Fisher's runaway, especially since the walk-toward outcome requires less extreme genetic assumptions and so may be more probable than the runaway. Following a number of authors (e.g., Grafen 1990; Wedekind 1994; Ritchie 2007; Danchin et al. 2008; Hoglund and Alatalo 2014), we refer to the process described by the basic model as the Fisher-Lande process (FLP).

To achieve our goal of testing the FLP with data from sexual radiations, we use a modified version of the basic model. First, we accept the argument of Pomiankowski (1987) and many subsequent authors that selection is likely to act on female mating preferences. We follow the standard convention of modeling stabilizing selection on preferences (e.g., Kirkpatrick 1985, 1996; Pomiankowski et al. 1991; Iwasa and Pomiankowski 1995; Day 2000), but we use a Gaussian form so that selection on the preference can be related to natural selection on the male trait. Second, we allow drift as well as selection to act on the traits (Lande 1981; Uyeda et al. 2009). This model feature is an antidote to selection

* Corresponding author; e-mail: arnolds@science.oregonstate.edu.
† ORCID: Arnold, http://orcid.org/0000-0001-9934-9111.

Am. Nat. 2016. Vol. 187, pp. 000–000.
DOI: 10.1086/686258

on preference, which will tend to drive the population to point equilibria and so eliminate the possibility of a sexual radiation (Lande 1981; Kirkpatrick 1982; Lande and Arnold 1985). Third, we model multiple male traits and multiple preferences so that we might account for the multivariate nature of sexual radiations.

The combination of multiple traits and selection on preferences is relatively unusual in the quantitative genetic modeling literature. Pomiankowski and Iwasa (1993, 1998) explored models of this type (without drift), but their goal was to define the conditions for perpetual evolution via stable limit cycles. Because of that goal, they employed unusual forms for stabilizing selection on traits and preferences that cannot be easily related to the empirical literature on selection. We are skeptical that stable limit cycles provide a general explanation for sexual radiations because in the context of the FLP they require unusual forms of selection that are unprecedented in the empirical literature as well as a delicate and implausibly fragile balance of parameter values. For these reasons, we sought a general explanation of sexual radiation using stochastic versions of the quantitative genetic theory that produce perpetual evolution.

Our specific goals are to (1) specify a modified version of the basic model of the FLP that relaxes three assumptions (infinite population size, single traits in both sexes, no selection on preferences), (2) explore the properties of that model with computer simulations, and, finally, (3) assess the ability of the model to account for sexual radiation using the example of birds of paradise and (4) use the OUwie model testing framework (Beaulieu et al. 2012) to estimate key parameters of the FLP.

We refer to our version of the basic model as the phenotypic tango model because the ornament and preference means of a lineage appear to dance through time. A molecular version of this multivariate process, termed the molecular tango, describes the perpetual coevolutionary dance of male and female proteins but without the benefit of a formal model (Palmer et al. 2005, 2007, 2010; Symonds and Elgar 2008; Wyatt 2014).

In the following discussions, we follow the common tradition of referring to the male traits that are the focus of female mate choice as "ornaments." By this evocative shorthand, we refer to any male trait that affects the probability of successfully mating with the female (e.g., genitalia) as well as elaborate plumage. Likewise, the corresponding female mating "preference" is shorthand for any aspect of behavior, physiology, or morphology that interacts with particular ornament(s) and affects the success of the sexual interaction (i.e., sperm transfer resulting in progeny production).

We outline an approach using multiple models that should be generally applicable to the analysis of tree-based data on male ornaments that are continuously distributed within and among populations. We use a sexual radiation in birds of paradise to illustrate this general approach. We show that a model of the FLP can be used to account for both the quantitative and the qualitative details of the sexual radiation in these birds. We also show that testing frameworks that discriminate between alternative models of process can be used to analyze sexual radiations. These successes argue that much can be learned about the sexual radiations by using analytical approaches that take into account inheritance, selection, drift, and phylogeny. Before detailing our modeling approach, we first review some relevant aspects of bird of paradise biology that motivate some modeling choices.

Birds of paradise have evolved extraordinary diversification in male plumage and behavioral displays over a period of about 26 million years (Irestedt et al. 2009). Plumage modifications are extensive in both morphology and coloration, often in ways unprecedented in the entire history of birds (Scholes 2008; Laman and Scholes 2014). The extraordinary male plumage of birds of paradise is presented to the female in intricate displays, during which the male adopts characteristic postures that reveal hidden features of plumage (Dinsmore 1970; Firth 1976; LeCroy 1981; Pruett-Jones and Pruett-Jones 1990). Throughout the radiation, displaying males use plumage and abrupt changes in posture to suddenly create novel, colorful shapes, behavioral events known as shape-shifting (fig. 1). During shape-shifting, the displaying male suddenly creates a static shape with his plumage and then bounces, rocks, or hops in a repetitive pattern that may continue for several minutes. Unique vocalizations often accompany the static and dynamic stage of display (Scholes 2008). Female choice is almost certainly the primary force that drives the remarkable display radiation of birds of paradise. Pulling all these facets of display history together, we see a pattern of perpetual evolution in many coordinated features of male plumage, behavior, and vocalization that informs our modeling effort. These three display features are organized in functional complexes that create ever-evolving static and moving displays that apparently affect the sexual receptivity of the female. With this context in mind, we pose our central question: What model of phenotypic evolution can explain the sexual radiation of birds of paradise? A leading contender in that search for explanation is the FLP, often and misleadingly known as the runaway process.

Methods

Description of the Phenotypic Tango

Our model for the phenotypic tango is based on Lande's (1981) model for the coevolution of sex-limited phenotypic traits. Several detailed explications of that model are avail-

Figure 1: Two male birds of paradise (*Paradisaea apoda*) displaying to a female, showing the role of the wings and tail in forming a static shape (from a photograph by Tim Laman in Laman and Scholes [2014]). A video by Tim Laman of events surrounding the image shown here is available at https://www.facebook.com/Birds.Lovers.1/videos/1003571246388699/.

able (Maynard Smith 1982; Arnold 1983, 1985; Mead and Arnold 2004; Kuijper et al. 2012), so only an abbreviated account is provided here. Our model closely follows Lande's model in assumptions, formulation, and notation, with four important exceptions (app. A). First, we model the evolution of two traits in each sex instead of just one so that evolution proceeds in a two-dimensional trait space, or "dance floor." Second, we allow stabilizing natural (e.g., viability) selection on preference as well as on ornament, whereas in the original Lande model only the ornament experienced stabilizing natural selection. Third, as in Lande (1981) but unlike in most quantitative genetic models of sexual coevolution, we allow the population to be finite in size. Consequently, the trait means tend to drift away from their natural selection optima every generation. The consequences of finite population size have been thoroughly explored in related Ornstein-Uhlenbeck (OU) models (Lande 1976*b*, 1979), and we apply those results to our system (app. A). Finally, we allow the natural selection optima for preferences to move as a function of time. For simplicity, we use a Brownian motion (BM) model for that bivariate movement.

We will often plot the results of our model in two dimensions even though we model the evolution of four traits. Imagine two continuously distributed male ornaments that are the focus of female mate choice. Likewise, imagine that the preferences for those ornaments are two continuously distributed female traits. Because each female most prefers to mate with a male with particular ornament values (e.g., a tail length of 20 cm and a wing length of 10 cm), we can plot her two preference values and the ornament values for that particular male in the same two-trait space. When the two points representing the ornament and preference are close together, mating is likely to occur between the male and female mating partners with those trait values. Conversely, when values for ornament and preference are far apart in trait space, mating is less likely. A variety of states for both ornaments and preferences exist in a population of males and females. We can summarize the entire population of mating partners by plotting the means for ornaments and preferences in the same way that we plotted the positions of states for individual males and females. We also can visualize the coevolution of ornament and preference as the movement of bivariate trait means in our two-trait space. In the next few sections, we present a formal version of this model, which will be needed to make quantitative predictions that can be tested with data.

Our model assumes that the phenotypic values of the two ornaments (z_1 and z_2) as well as the two preferences (y_1 and y_2) are the sums of genetic and environmental values. Genetic and environmental values are assumed to be independent and normally distributed. The model can accommodate any pattern of genetic correlation among the four traits (app. A), but for simplicity we will allow only one kind of between-sex correlation, that is, correlation between traits z_1 and y_1 and between z_2 and y_2.

Two selective forces drive the evolution of the ornaments (z_1 and z_2). First, bivariate stabilizing selection tends to pull the ornament means toward an intermediate natural (viability) selection optimum. This stabilizing selection is modeled with a Gaussian (bell-shaped) function with a width

parameter (ω_{zii}) analogous to a variance. This selection slightly restricts the statistical availability of ornaments to preferences. Second, the two preference traits (y_1 and y_2) exert directional sexual selection on the ornaments. Each female is most inclined to mate with a male whose ornaments z_1 and z_2 most closely match, respectively, the values of her preferences y_1 and y_2. In other words, her preferences are absolute rather than relative (Lande 1981). Her tendency to mate with a male is modeled as a bivariate Gaussian function with personal optima given by y_1 and y_2 and a width parameter ν_{ii} that is common to all females. The more the male's ornament departs from her personal optimum, the less likely she is to mate with him. From these assumptions, one can compute the total force of sexual selection on each of the ornaments (app. A). Furthermore, as shown by Lande (1981), the combination of assortative mating (i.e., between z_1 and y_1 and between z_2 and y_2) and sexual selection creates linkage disequilibrium between certain ornament alleles and certain preference alleles. That disequilibrium in turn is expressed as a positive genetic covariance, B_{ii}, between the trait pairs z_1, y_1 and z_2, y_2.

Preferences (y_1 and y_2) experience only bivariate Gaussian stabilizing selection that tends to pull their means toward an intermediate bivariate natural selection (viability) optimum. This stabilizing natural selection (ω_{yii}) affects the availability of preferences to ornaments. This stabilizing selection can be stronger or weaker than the stabilizing selection that acts on ornaments. The bivariate optimum for preferences may be the same or different than the ornament optimum. Unlike the ornaments, however, preferences do not experience sexual selection. In other words, we assume that all surviving females mate; the preferences of a female do not affect her mating success or fecundity.

In the absence of sexual selection on the ornaments, the ornament mean will eventually attain an evolutionary equilibrium in which the average tendency to move toward the natural selection optimum due to stabilizing selection is balanced by an average tendency to drift away from the optimum. If we examine a large number of replicate populations that have attained this selection-drift balance, their bivariate ornament means will be normally distributed about the optimum (app. A). At equilibrium with uncorrelated ornaments, the variance among lineages in ornament mean is expected to be

$$\frac{\omega_{zii} + P_{ii}}{2N_e}, \tag{1}$$

where P_{ii} is the within-population phenotypic variance of the ith ornament and N_e is the within-lineage effective population size (Lande 1976*b*). In the absence of sexual selection, the bivariate preference mean will eventually achieve a similar equilibrium in which the preferences means of replicate lineages are normally distributed about the bivariate preference optimum. We might not expect either of these equilibria to be achieved if the ornaments experience sexual selection. But given the more complicated selection scheme in our model, how exactly does the equilibrium differ from simple drift-selection balance? We will present an analytical solution to this question based on the deterministic equations for the process. How rapidly is that more complicated equilibrium achieved? Normally this question would be answered with a stability analysis based on an analytical solution to the dynamic equations for a model such as ours. Unfortunately, we lack an analytical solution to the stochastic version of our model. Consequently, we will use computer simulations to answer fundamental questions about the dynamic properties of the phenotypic tango.

Simulation Procedures

Qualitative Predictions from the Phenotypic Tango Model. To explore the deterministic behavior of the model, we eliminated the stochastic contribution of drift to trait change each generation and then varied the contributions of starting position in trait space, the positions of the trait optima relative to one other, and the magnitude of genetic correlation between the sexes.

In using simulations to explore the model's stochastic behavior, we focused on parameters whose contributions to the phenotypic tango could not be predicted easily a priori (table 1). For example, because genetic variance increases rates of drift and responses to selection, we expect a priori that it will increase the tempo of the tango. We assume that genetic variances have equilibrated under the prevailing forces of mutation, drift, and selection (Lande 1976*a*; Bürger and Lande 1994; Jones et al. 2003), and consequently we fix the genetic variance of each of the four traits at an intermediate, empirically observed value of 0.4 (Estes and Arnold 2007). In contrast, the relative strengths of stabilizing selection (ω_{zii} and ω_{yii}) and mate preference (ν_{ii}) have less obvious effects on the anticipated tango. Consequently, we examined the effects of these parameters in some detail. In each computer run, we exposed 25 or 100 independent, replicate populations to the same parameter values and followed the evolution of bivariate ornament and preference means for 500 generations. Preliminary runs revealed that 500 generations was generally sufficient for the trait means of replicate lineages to achieve an equilibrium pattern under most of the combinations of parameter values that we explored, but in exceptional cases tens of thousands of generations were required and simulations were run for 100,000 generations (table 2). For simplicity and ease of interpretation of results, we employ a set of standard conventions. For example, in most runs we let natural selection optima coincide for ornaments and preferences and started all replicate lineages at that same point in trait space.

Table 1: Values of parameters used in simulations

Description	Symbol	Values
Phenotypic variance within the sexes	P_{ii}, Q_{ii}	1
Genetic variance within the sexes	G_{ii}, H_{ii}	.04, .4
Genetic covariance between the sexes	B_{ii}	0, .24, .36
Natural selection optima	θ_{zi}, θ_{yi}	0, .2, .3, .5, .75
Natural selection width, ornament	ω_{zii}	4, 9, 19, 29, 49, 99, 999
Correlational natural selection, ornament	ω_{zij}	0, 3.5, 7.5
Natural selection width, preference	ω_{yii}	4, 9, 19, 29, 49, 99, 199, 299, 499, 999, 9,999, 99,999
Correlational natural selection, preference	ω_{yij}	0, 7.5, 25
Strength of female mate choice	ν_{ii}	.08, .4, .8, 5, 10, 20, 40
Correlational female mate choice	ν_{ij}	0, .3
Effective population size	N_e	500, 1,000, 5,000
Variance of preference natural selection optimum	σ^2_θ	.000055

We summarized the results of each run in a generation-by-generation animation that enabled us to rapidly assess the effects of a change in one or more parameters. We use 95% confidence ellipses to portray the outcomes expected for ornament and preference means in the absence of sexual selection. These ellipses represent the dance floors that we would expect in the absence of mate choice. Under that condition, 95% of replicate lineage means are expected to reside within the boundaries of the ellipse. As time unfolds from starting conditions, replicate lineage means spread out, away from the natural optimum as they move toward a drift-stabilizing selection balance. The 95% confidence ellipse expands as time proceeds and then achieves a final equilibrium size (app. A). We portray the temporally expanding ellipse with a narrow line and the final equilibrium ellipse with a bold solid line. We also show the 95% confidence ellipses for the evolving clouds of ornament and preference means with narrow lines. These data ellipses are usually not perfect circles and so can be distinguished from the expected 95% confidence ellipses. Turning to results that were apparent in animations of our computer runs, we first consider the evolutionary trajectories of an individual lineage responding to drift and selection and then turn to trajectories of sets of 25 or 100 replicate lineages. Animated versions of the static figures that follow can be viewed at http://phenotypicevolution.com/?p=221. A summary of the parameters used in the figure simulations is provided in table 2. An example of R script used to produce the figures is provided in the Dryad Digital Repository: http://dx.doi.org/10.5061/dryad.66ft5.2 (Arnold and Houck 2016).

Quantitative Tests of the Phenotypic Tango Model Predictions. Published data on bird of paradise morphology in combination with a published time-calibrated phylogeny were used to gauge the rate and extent of ornament diversification. In this section and the next, we focus on morphological ornaments because data on preference are seldom available for sexual radiations (but see Grace and Shaw 2011). Data on wing, tail, and tarsus length of plumed males and females in 14 populations representing all seven species in the genus *Paradisaea* were obtained from Lecroy (1981; data file deposited in the Dryad Digital Repository: http://dx.doi.org/10.5061/dryad.66ft5.2 [Arnold and Houck 2016]). Population means for each sex-population combination were standardized by dividing the raw means (mm) by within-sex-population standard deviations. Standard errors for each mean were computed from the data provided by Lecroy (1981) and used in the OUwie analysis. The timescale for ornament diversification was estimated from a time-calibrated phylogeny of the family Paradisaedae (15 genera) based on mitochondrial and nuclear gene sequences (Irestedt et al. 2009).

Quantitative Tests Using the Program OUwie. We used OUwie (Beaulieu et al. 2012) to compare fits of OU and BM processes to the *Paradisaea* data and to estimate FLP parameters (data and tree files are available at the Dryad Digital Repository:http://dx.doi.org/10.5061/dryad.66ft5.2 [Arnold and Houck 2016]). The OUwie program uses a generalization of Hansen's (1997) model for a quantitative traits evolving by an OU process as well as the standard model for evolution by BM (Beaulieu et al. 2012). The program allows the user to specify two or more selection regimes on a phylogeny and estimates separate process parameters corresponding to those regimes. As a quantitative trait evolves by OU along a branch of a phylogeny, the change in its mean at generation t in the kth selection regime is given by the following stochastic differential equation:

$$d\bar{z}_k(t) = \alpha[\theta_k - \bar{z}_k]dt + \sigma\, dBM_k(t), \qquad (2)$$

where θ_k is the trait optimum in the kth selection regime and the last term on the right represents a contribution from a

Table 2: Values of parameters used in figure simulations

Figure	Pop	N_e	Gen	Orn/pref	$\boldsymbol{\omega}_z$	$\boldsymbol{\omega}_y$	$\boldsymbol{\theta}_z$; $\boldsymbol{\theta}_y$	$\boldsymbol{\nu}$	**G, H**	**B**	σ^2_θ
3	1	500	500	Orn	4, 0, 0, 4	NA	0, 0	NA	.4	NA	NA
4*A*	100	5,000	500	Both	4, 0, 0, 4	19, 0, 0, 19	0, 0; .5, .5	.4	.4	0	NA
4*B*	100	5,000	500	Both	4, 0, 0, 4	19, 0, 0, 19	0, 0; .5, .5	.4	.4	.24	NA
4*C*	100	5,000	500	Both	19, 0, 0, 19	4, 0, 0, 4	0, 0; .5, .5	.4	.4	.24	NA
4*D*	100	5,000	500	Both	9, 7.5, 7.5, 9	29, 25, 25, 29	0, .2; .4, .3	.4, .3	.4	.24	NA
6	25	500	10^2 K	Both	9, 0, 0, 9	9,999, 0, 0, 9,999	Same	.4	.4	.24	NA
7	25	5,000	10^2 K	Both	9, 0, 0, 9	19, 0, 0, 19	Same	.4	.4	.24	5.5×10^{-4}
B1*A*	100	5,000	500	Both	4, 0, 0, 4	9, 0, 0, 9	Same	.4	.4	.24	NA
B1*B*	100	5,000	500	Both	4, 0, 0, 4	99, 0, 0, 99	Same	.4	.4	.24	NA
B2*A*	100	5,000	500	Both	9, 0, 0, 9	299, 0, 0, 99	Same	.4	.4	.24	NA
B2*B*	100	5,000	500	Both	29, 0, 0, 399	49, 0, 0, 49	Same	.4	.4	.24	NA
B3*A*	100	5,000	500	Both	9, 0, 0, 9	99, 0, 0, 99	Same	.4	.4	0	NA
B3*B*	100	5,000	500	Both	9, 0, 0, 9	99, 0, 0, 99	Same	.4	.4	.36	NA
B4*A*	100	5,000	500	Both	4, 0, 0, 4	99, 0, 0, 99	Same	40	.4	.24	NA
B4*B*	100	5,000	500	Both	4, 0, 0, 4	99, 0, 0, 99	Same	.08	.4	.24	NA
B5*A*	25	500	10^2 K	Both	9, 0, 0, 9	9,999, 0, 0, 9,999	Same	.4	.4	.24	NA
B5*B*	25	500	10^2 K	Both	9, 0, 0, 9	9,999, 0, 0, 9,999	Same	.4	.4	.24	NA
B5*C*	25	500	10^2 K	Both	9, 0, 0, 9	9,999, 0, 0, 9,999	Same	.4	.4	.24	NA
B5*D*	25	500	10^2 K	Both	9, 0, 0, 9	9,999, 0, 0, 9,999	Same	.4	.4	.24	NA
B5*E*	25	500	10^2 K	Both	9, 0, 0, 9	9,999, 0, 0, 9,999	Same	.4	.4	.24	NA
B6	1	500	500	Orn	4, 0, 0, 4	NA	0, 0	NA	.4	NA	5.5×10^{-4}

Note: Elements of the 2×2 matrices in columns 6 and 7 are presented in the order x_{11}, x_{12}, x_{21}, and x_{22}. One value for $\boldsymbol{\nu}$ represents the value of the two diagonal elements; off-diagonal elements are 0. Two values for $\boldsymbol{\nu}$ represent the values of elements ν_{11} and ν_{12} in a symmetric 2×2 matrix. Single values for **G**, **H**, and **B** represent the diagonal elements of 2×2 matrices; off-diagonal elements are 0. Ornament and preference are abbreviated "orn" and "pref"; populations and generations are abbreviated "pop" and "gen."

BM process, equal to a draw from a normal distribution with a mean of 0 and variance of σ^2 (Beaulieu et al. 2012). Each generation, a restoring force $\alpha = G_{ii}/(\omega_{zii} + P_{ii})$, where G_{ii} is additive genetic variance for the trait, pulls the trait mean toward the optimum (Lande 1976*b*).

As the restraining force α approaches 0, expression (2) describes BM:

$$\mathrm{d}\bar{z}_k(t) = \sigma \, \mathrm{d}BM_k(t). \tag{3}$$

Two biological interpretations for the BM process have been described (Felsenstein 1985). Under one interpretation, the BM process is genetic drift of the trait mean, in which case $\sigma^2 = G_{ii}/N_e$, such that the distribution of replicate lineage means is normally distributed with a mean of 0 (or the ancestral mean) and a variance of tG_{ii}/N_e at generation t (Lande 1979). The other interpretation is that the BM process is the motion of the trait mean as it tracks an optimum that undergoes BM, in which case the limiting distribution of replicate lineage trait means will be normally distributed with a mean of 0 (or the ancestral mean) and a variance that converges on

$$\frac{\sigma^2_\theta + G_{ii}/N_e}{2\alpha} + t\sigma^2_\theta \approx t\sigma^2_\theta, \tag{4}$$

where σ^2_θ is the per generation variance in the position of the optimum, α is the restoring force given above, and t is the number of elapsed generations (app. A; Hansen et al. 2008). In summary, expression (3) describes a BM process, with a parameter σ^2 that estimates G_{ii}/N_e under the genetic-drift-of-the-mean interpretation or estimates σ^2_θ under the Brownian-motion-of-the-optimum interpretation.

Standard errors of the OUwie parameters α and σ^2 were estimated by bootstrapping (1,000 replicates) using function owie.boot. That procedure included drawing samples from the sampling distribution of the trait (using standard errors of the mean provided for each of 14 populations) as well as over hypothetical phylogenetic trees. Standard errors of each population trait mean were also included in calculations leading to model comparisons. This inclusion reduced calculation bias favoring the OU model with higher rates in the younger regime, which arises because one regime is nested inside the other. Standard errors of OUwie parameter θ were estimated from expressions given by Beaulieu et al. (2012). Under OU models, θ represents the trait optimum in one or more selection regimes. Under BM models, θ represents the ancestral mean at the root of a clade or the entire tree.

In simulations of the phenotypic tango model with a moving natural selection optimum, a draw each genera-

tion from a bivariate normal distribution with a mean of 0 and a variance of σ_θ^2 was added to the position of the optimum in the preceding generation. This procedure was used to produce BM of the natural selection optimum.

Tree topology and branch lengths from Irestedt et al. (2009) were used to define a tree for the genus *Paradisaea* with tip taxa corresponding to the 14 taxa in the LeCroy (1981) data set (fig. 2). The Irestedt et al. (2009) tree (their fig. 2) provided only six time-calibrated nodes for the genus *Paradisaea*, whereas the tree used in the OUwie analysis had nine nodes. Three new nodes were created by creating polytomies for three taxa (*minor*, *apoda*, *raggiana*) that were represented by two to four populations (subspecies) in LeCroy's (1981) data, placing those polytomies halfway between the tips and the closest time-calibrated node.

To determine whether adaptive peak movement would improve model fits, we designated two selection regimes on the *Paradisaea* tree (fig. 2). One regime included the common ancestor of the genus (dated at 9.4 Ma) and four basal taxa (*rudolphi*, *guilielmi*, *rubra*, *decora*). The other regime included three taxa (*minor*, *apoda*, *raggiana*) and their common ancestor, dated at 1.4 Ma. In other words, our designation supposes that one selection regime prevailed at the origin of the genus in the middle Miocene and continued to the present time, affecting four species, and that another began in the middle Quaternary, affecting a monophyletic set of three species.

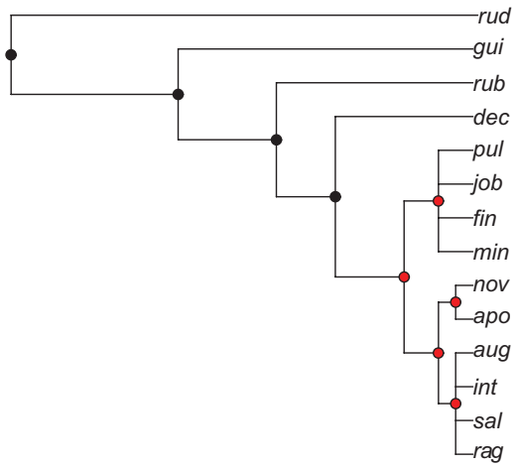

Figure 2: Phylogeny of 14 populations of *Paradisaea* used in the OUwie analysis, based on the results of Irestedt et al. (2009). The tip taxa are *P. rudolphi*, *P. guilielmi*, *P. rubra*, *P. decora*, *P. minor pulchra*, *P. minor jobiensis*, *P. minor finschi*, *P. minor minor*, *P. apoda novaeguinaea*, *P. apoda apoda*, *P. raggiana augustaevictoriae*, *P. raggiana intermedia*, *P. raggiana salvadorii*, and *P. raggiana raggiana*. The estimated ages of nodes are (from left to right) 9.4, 6.0, 4.0, 2.8, 1.4, 0.7, 0.7, 0.35, and 0.35 Ma. Two hypothetical selective regimes are denoted with node colors (black and red).

Results

Qualitative Predictions from the Phenotypic Tango Model

In the absence of drift, the equilibrium for the full process with natural and sexual selection is a single point that is stable under the sets of parameters used in the simulations (app. A). At this point equilibrium the preference means are at their natural selection optima. But if the natural selection optima differ between the sexes, the ornament means are pulled away from their natural selection optima by sexual selection so that they equilibrate along a line connecting the natural selection optima of preferences and ornaments. Strong sexual selection (small ν) pulls the ornament optimum toward the preference optima, and strong natural selection on ornaments (small ω_{zii}) pulls the ornament mean toward the ornament optimum. To follow the following descriptions of stochastic results, the reader should consult the online animations (http://phenotypicevolution.com/?p=221) as well as the static figures; otherwise, the language used to describe the results may be enigmatic. Supplemental figures are provided in appendix B (available online).

With drift but in the absence of sexual selection, the bivariate ornament mean chaotically meanders in the immediate vicinity of its optimum. Bounds on the trajectory of the mean are well described by the 95% confidence ellipse imposed by natural selection (fig. 3). In other words, diversification of the ornament (or preference) is affected only by natural selection (ω_{zii} or ω_{yii}) and drift (via N_e) in the absence of sexual selection, as expected from expression (1).

Sexual selection causes both ornaments and preferences to diversify beyond the limits imposed by natural selection and drift. The ordinary evolution (i.e., in the absence of sexual selection) of the ornaments and preferences (fig. 4*A*) lies within the boundaries described by their natural selection 95% confidence ellipses. If we allow mate choice, both sets of traits undergo extraordinary evolution, but the ornaments especially do, because they experience direct sexual selection (fig. 4*B*). When the positions of the ornament and preference optima differ, as in figure 4*B*, the ornament means are pulled toward the preference mean and a stable cloud of moving means is formed between the two optima. In contrast, the preference means form a stable cloud of moving values that are centered over the preference optimum. If the conditions of stabilizing selection in figure 4*B* are reversed so that stabilizing selection is weak on the ornaments but strong on the preferences, extraordinary diversification of the ornaments is completely suppressed (fig. 4*C*). Indeed, under these conditions the evolution of the ornaments is hyperconservative, such that trait means perpetually reside within the stringent limits imposed by natural selection on the preferences. If the correlational

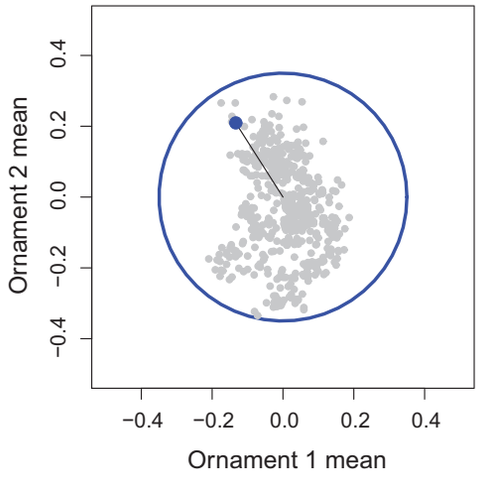

Figure 3: Evolution of male ornaments is restrained when sexual selection is absent. The two axes are measurements for two ornament traits, scaled in units of within-population phenotypic standard deviation ($P^{1/2}$). The evolution of a single lineage mean is illustrated over the course of 500 generations in gray. The bivariate mean of the two traits at generation 500 is shown as a blue dot. The 95% confidence ellipse for diversification by natural selection is shown in blue. A black line connects the bivariate mean to the natural selection optimum. Past positions of the mean are shown as gray dots. Other parameter values: $N_e = 500$; $\omega_z = 4, 0, 0, 4$; $P_{ii} = 1$; $G_{ii} = 0.4$.

natural selection acts on both ornaments and preferences, then the ornaments and preferences have equilibrium dance floors that are inclined ellipses (fig. 4*D*). Consequently, in the discussions that follow we shall be concerned with the situation in which preferences experience weaker natural selection than the ornaments ($\omega_{yii} \gg \omega_{zii}$), that is, the natural selection ellipse for preferences is larger. Under these conditions, ornament evolution will be extraordinary, and we can ask which factors promote that exceptional diversification. We will also focus on the case in which the optima of ornaments and preferences coincide so that we can concentrate on the conditions that affect the size of the sexual radiation rather than its location.

Mate choice can cause the ornament mean to evolve far away from its natural selection optimum. Meandering of the ornament mean outside the limits imposed by natural selection alone is especially dramatic when natural selection is weaker on the preferences than on the ornaments (as is almost certainly the case when the ornaments are morphological and the preferences are behavioral). Adding mate choice also produces the phenotypic tango that we anticipated. In particular, sexual selection causes the bivariate means of ornaments and preferences to move together (dance) in trait space (fig. B1*A*; figs. B1–B6 are available online). As we relax natural selection on the preferences (i.e., make ω_{yii} larger), the dance floor expands, and the dancing preference pulls the ornament mean farther away from its natural selection optimum (fig. B1*B*). Mate choice also exaggerates the evolution of the preferences away from their natural selection optimum. At equilibrium, pairs of preference and ornament means evolve chaotically on dance floors that are substantially larger than the limits imposed by natural selection alone.

Asymmetry in natural selection as well as correlational selection on the preferences affects the shape as well as the size of the dance floor. For example, by making stabilizing selection on one preference trait stronger, we change the shape of the dance floor from circular to oval (fig. B2*A*). A comparable asymmetry in functional constraints on the ornaments has no effect on the shape of the dance floor (fig. B2*B*).

In the absence of a genetic correlation between the sexes, the evolving preference means pull the ornament means away from their optimum, but preference diversification falls within limits set by natural selection (fig. B3*A*). When genetic covariance is 0 ($B_{ii} = 0$), the terms describing correlated responses vanish (app. A), and preference evolution is ordinary. In other words, correlated response to selection mediated by genetic correlation is a necessary ingredient for extraordinary evolution of the preference mean (fig. B3*B*).

The size of the radiation as well as its tempo are directly affected by the strength of mate choice. The strength of choice is governed by the width of the Gaussian function that specifies how stringently the female attends to the ornaments of the male. When that function is wide (large ν_{ii}), preferences are forgiving, and a female will mate with males whose ornaments deviate substantially from her personal optimum. When mate choice is sufficiently weak (large ν_{ii}), preferences remain inside their 95% natural selection ellipse (fig. B4*A*). But when the function is narrow (small ν_{ii}), the female mates only with males whose ornaments are very close to her optimum. As the strength of sexual selection is increased (by decreasing the value of ν_{ii}), ornament-preference pairs dance faster and closer together (fig. B4*B*). In other words, the dance floor collapses in size as we decrease the strength of mate choice.

To appreciate the coordinated nature of male and female trait coevolution, it helps to plot the lineage mean of one preference (y_1) as a function of the lineage mean of the corresponding ornament (z_1). In such a plot, we see that coevolution proceeds along a line of equilibrium (fig. B5), similar to the one described by Lande (1981). As in Lande's (1981) model, selection drives the bivariate lineage mean toward this line so that the ornament mean of a lineage in any given generation is very close to a mirror image of that lineage's preference mean. The similarity of the images is astoundingly large; the overall correlation between the means of ornament 1 (z_1) and preference 1 (y_1) in the 100,000 generations of simulation reported in figure B5 (25 replicate

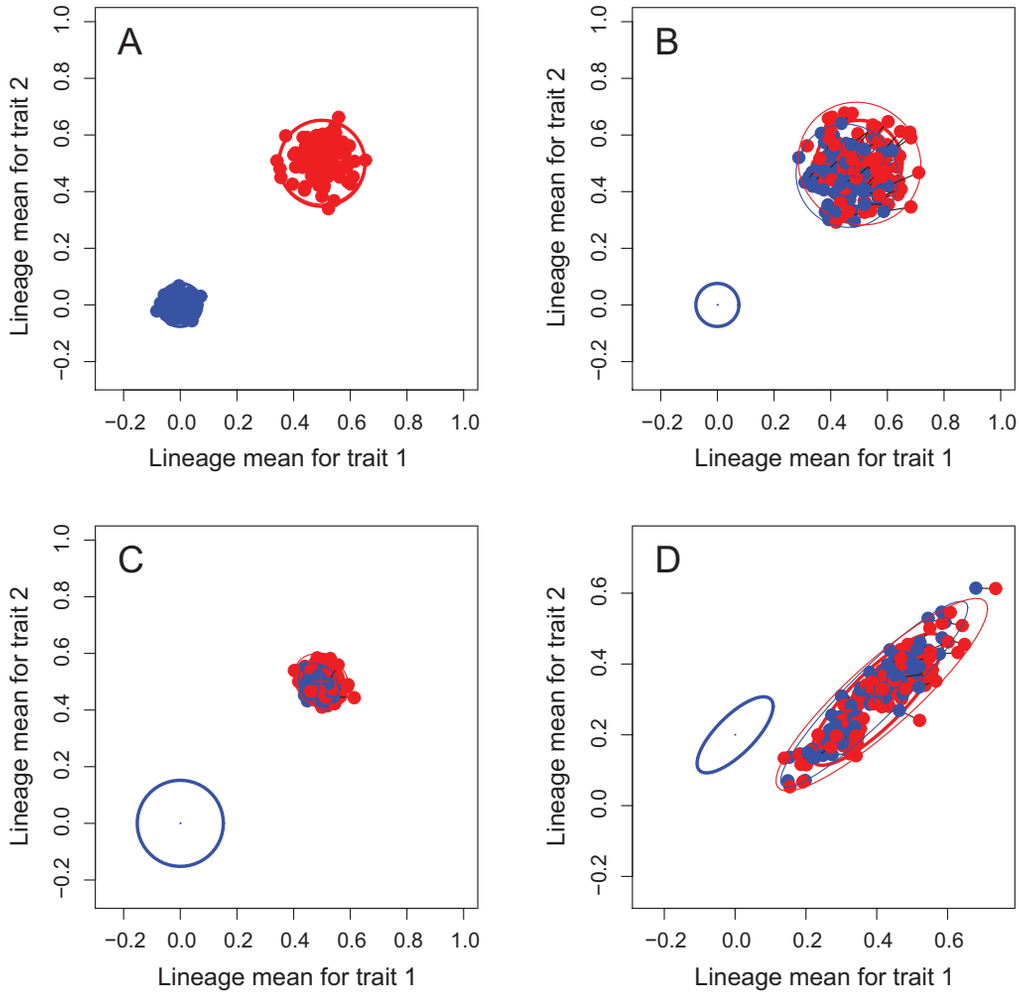

Figure 4: Sexual selection exaggerates the evolution of ornaments and mating preferences, producing a phenotypic tango (illustrated with sets of 100 lineages at generation 500; $N_e = 5{,}000$; $P_{ii} = Q_{ii} = 1$; $G_{ii} = H_{ii} = 0.4$; $B_{ii} = 0.24$; $\nu_{ii} = 0.4$; $\nu_{ij} = 0$). The 95% confidence ellipses for diversification of ornaments and preferences by natural selection alone are shown as heavy blue and red ellipses, respectively. The 95% confidence ellipses for the sample of ornament and preference means are shown as light blue and red ellipses, respectively. *A*, Evolution of ornaments and preferences in the absence of sexual selection ($\omega_z = 4, 0, 0, 4$; $\omega_y = 19, 0, 0, 19$; $\theta_z = 0, 0$; $\theta_y = 0.5, 0.5$; $B_{ii} = 0$). *B*, The evolution of ornaments and preferences in the presence of sexual selection is a tango ($\omega_z = 4, 0, 0, 4$; $\omega_y = 19, 0, 0, 19$; $\theta_z = 0, 0$; $\theta_y = 0.5, 0.5$; $B_{ii} = 0.24$). The positions of ornament and preference means for a particular lineage are shown as blue and red dots, respectively, connected by a black line. *C*, When stabilizing selection on ornaments and preferences is reversed (weak on ornaments, strong on preferences), extraordinary evolution of ornaments is eliminated ($\omega_z = 19, 0, 0, 19$; $\omega_y = 4, 0, 0, 4$; $\theta_z = 0, 0$; $\theta_y = 0.5, 0.5$; $B_{ii} = 0.24$). *D*, Correlational natural selection on ornament and preference changes their 95% confidence ellipses from circles to inclined ellipses ($\omega_z = 9, 7.5, 7.5, 9$; $\omega_y = 29, 25, 25, 29$; $\theta_z = 0, 0.2$; $\theta_y = 0.4, 0.3$; $B_{ii} = 0.24$; $\nu_{11} = \nu_{22} = 0.4$; $\nu_{12} = \nu_{21} = 0.3$).

lineages) was 0.99992. In other words, on average the evolving preferences accounted for 99.98% of the variance in coevolving ornaments. This observation that ornament evolution mirrors preference will be important to us when we turn to actual data on birds of paradise because the implication of figure B5 is that we can accurately deduce preference evolution from observed ornament evolution or vice versa.

Explaining Birds of Paradise with the Phenotypic Tango Model

To view the sexual radiation of birds of paradise through the lens of the phenotypic tango model, we will restrict our attention to 14 populations representing seven species in the genus *Paradisaea*. This restriction is necessary because only for this genus do we have data on epigamic traits mea-

sured in both males and females and in multiple species (LeCroy 1981). How extensive is the evolution of display traits in this genus?

A summary of relevant data (data file available in the Dryad Digital Repository: http://dx.doi.org/10.5061/dryad.66ft5.2 [Arnold and Houck 2016]) reveals that for two male traits that figure prominently in male courtship displays, wing and tail lengths, the 95% confidence limits for the width of the radiation are ± 10.7 and 12.4 within-population phenotypic standard deviations ($P^{1/2}$; fig. 5). For females, the wing and tail values are ± 4.9 and $2.0P^{1/2}$. The females' values are inside the limits normally seen for divergence of size-related traits on a timescale of 9 million years, the estimated age of the genus (Estes and Arnold 2007; Irestedt et al. 2009; Arnold 2014). Likewise, the radiation widths for tarsus length (a trait only marginally involved in displays) in males and female are ± 5.2 and $0.8P^{1/2}$, respectively. In other words, we can conclude that the evolution of male display characters is indeed extraordinary in extent, whereas the evolution of homologous traits in females and nondisplay traits in both sexes is not extraordinary. Notice that our focus is on the extent of evolution, not its rate, a point to which we will return in "Discussion."

We can appreciate both the pattern and the extent of display trait evolution in figure 5 by comparing it to one of our simulation scenarios (fig. 4*D*). Trait evolution appears to be positively correlated in both sexes (fig. 5), but the bivariate wing mean of males is about $10P^{1/2}$ greater than that of females, and the bivariate tail mean of males is about $5P^{1/2}$ greater than that of females. The pattern evident in figure 5 is similar to the pattern we see in figure 4*D*, in which we plotted the 95% confidence limits for evolution by natural selection acting on two male ornaments (blue) and on corresponding preferences (red). Under the phenotypic tango model (see Lande and Arnold 1985), we expect the blue ellipse in figure 4*D* to be closely similar to the ellipse for homologous female traits under natural selection (i.e., similar to the blue ellipse in fig. 5). Likewise, as we argued at the end of the preceding section, we expect the male ornament ellipse in figure 5 to mirror the female preference ellipse for these lineages. But how can we account for the positive inclination of the ellipses in figure 5? To produce those inclinations, we must assume that positive correlational selection acts on both ornaments and preferences ($\omega_{12} > 0$). Making those assumptions, the phenotypic tango model can produce a pattern of trait radiation (fig. 4*D*) very much like the one observed in birds of paradise (fig. 5). Can the model also produce the quantitative aspects of the pattern?

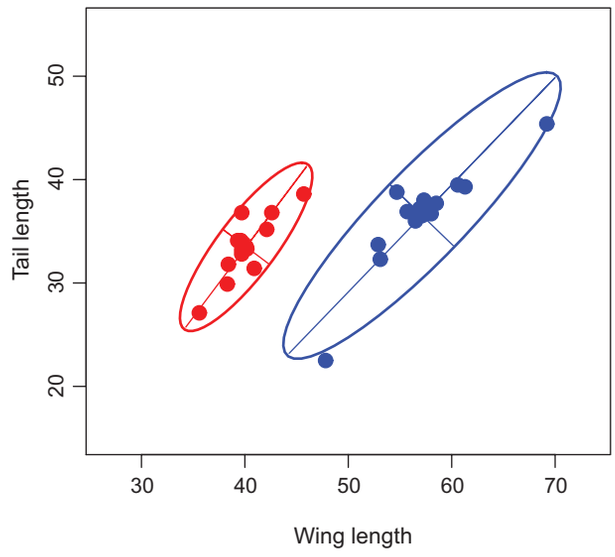

Figure 5: Tail length as a function of wing length in 14 populations of birds of paradise, representing seven species in the genus *Paradisaea*. Measurements are expressed in units of average within-population standard deviation ($P^{1/2}$). Females and males are indicated by red and blue dots, respectively; 95% confidence ellipses and principal axes are shown for each sex.

A challenge in testing the phenotypic tango model with the *Paradisaea* data is that we need to account for an ornament radiation width of approximately ± 10–$12P^{1/2}$ over a period of 9 million years or, using an estimated generation time of 5 years, 1.8 million generations. Exploring the model with computer simulations revealed two conditions that could produce such an extensive radiation on a relatively short timescale: either very weak stabilizing selection on preferences or modest movement per generation of the natural selection optimum for preferences. Figure 6 shows an example of a radiation comparable to wing length in birds of paradise produced by specifying very weak selection on preferences. In this example, we see divergence greater than ± 10–$12P^{1/2}$ in about 20,000 generations. We also see that the limits of extraordinary divergence in ornaments produced by sexual selection can be approximated by doubling the 99% confidence limits expected when preference evolves under natural selection alone (see the red dotted lines in fig. 6). This figure also illustrates the faithful mirroring of preference evolution by ornaments, especially visible when the preference mean is far from its optimum.

The production of a radiation comparable to birds of paradise by letting the preference optimum move by BM is shown in figure 7. In this example, stabilizing selection on both preferences and ornaments is relatively strong, yet the radiation achieves the requisite extent in about 30,000–40,000 generations. The rate of movement of the preference optimum that produces this result is modest ($\sigma^2_\theta = 0.00055$), but the consequences are astounding on a timescale greater than 100,000 generations (see the orange lines in fig. 7). To appreciate the amount of movement produced each gen-

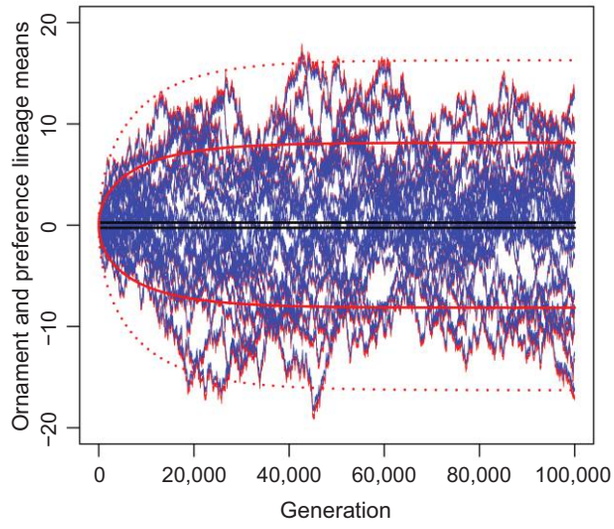

Figure 6: Simulated ornament and preference lineage means evolving for 100,000 generations, showing that ornament diversification is predicted by two times the natural selection confidence limits for preferences (illustrated with 25 lineages; $N_e = 500$; $P_{ii} = Q_{ii} = 1$; $G_{ii} = H_{ii} = 0.4$; $B_{ii} = 0.24$; $B_{ij} = 0$; $\nu_{ii} = 0.4$; $\nu_{ij} = 0$; $\omega_z = 9, 0, 0, 9$; $\omega_y = 9{,}999, 0, 0, 9{,}999$; at generation 100,000, these are the same data as in figure B5). Ornament (blue) and preference (red) means are shown in units of within-population standard deviation, $P^{1/2} = Q^{1/2}$. Black curves show the expected 99% confidence limits for ornament diversification by natural selection alone. Bold red lines show the expected 99% confidence limits for preference diversification by natural selection alone. Dotted red lines show two times the 99% confidence limits for preferences.

eration by this value of σ^2_θ, see figure B6, which portrays a simulation with the same parameter values as figure 3 but with the optimum moving.

Testing Alternative Models of Process with the Birds of Paradise Data

In the preceding section, we determined that we could explain the *Paradisaea* data with the phenotypic tango model, and we roughly bracketed the parameter conditions that would be required for that explanation. In this section, we use the OUwie model evaluation framework (Beaulieu et al. 2012) to compare generic versions of OU and BM processes and to estimate key parameters of the FLP (e.g., effective population size, stabilizing selection on preferences, rate of movement of the preference optimum). A key feature of OUwie is that selection regimes can be designated so that parameters of both OU and BM processes change at predetermined points on a phylogeny. In particular, we will use OUwie to determine whether peak movement in an OU model gives a better fit to the data than a stationary optimum. We will also use OUwie to determine which version of BM best describes the data, genetic drift of the ornament mean or BM of the preference optimum and, hence, of the ornament mean.

Parameter estimates obtained by fitting simple OU and BM models to the wing length data for *Paradisaea* males using package OUwie are shown in table 3. Analysis of tail and tarsus lengths in both sexes gave similar results and are not reported. The best-fitting model was BMS, which allows for different diversification rates in the two regimes but fits a single value to the trait means at the root of each regime. BMS is substantially better than BM1, which attempts to fit a single diversification rate across both regimes. OUM, which allows different optima in the two regimes but fits the same diversification rate and optimum in both, is somewhat worse than BMS but substantially better than other OU models that are either simpler (OU1) or more complex (OUMV). In other words, the best fitting models are relatively simple versions of BM or OU.

Table 4 shows the FLP parameter estimates derived from the parameters estimated by OUwie. For example, fitting the best-fitting OU model with a single selection regime (OUM) yields an estimate of the restoring force that pulls the wing length mean back toward its natural selection optimum of $\alpha = 12.49$. This restoring force is equivalent to $G_{ii}t/(\omega_{zii} + P_{ii})$, which we can use to estimate the stabilizing selection

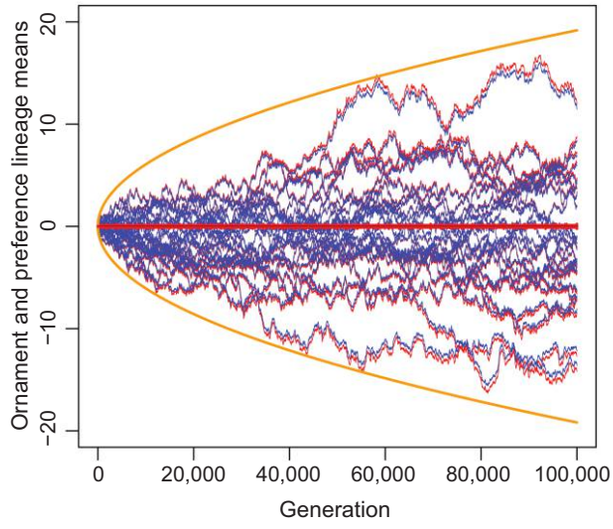

Figure 7: Simulated evolution of ornaments and preferences with a moving preference optimum (illustrated with a set of 25 lineages; $N_e = 500$; $P_{ii} = Q_{ii} = 1$; $G_{ii} = H_{ii} = 0.4$; $B_{ii} = 0.24$; $\nu_{ii} = 0.4$; $\nu_{ij} = 0$; $\omega_z = 9, 0, 0, 9$; $\omega_y = 9{,}999, 0, 0, 9{,}999$; $\sigma^2_\theta = 0.00055$). Conventions are as in figure 6. The 95% confidence limits for ornament diversification by natural selection alone are not visible. The orange curve shows the 95% confidence limits for diversification of preference means evolving under a model in which the preference optimum moves by Brownian motion.

Table 3: Ornstein-Uhlenbeck (OU) and Brownian motion (BM) model results for diversification in male *Paradisaea* wing lengths obtained using the package OUwie

	Model				
	BMS	OUM	OU1	OUMV	BM1
ΔAICc	.0000	1.1127	3.8031	4.2589	6.0834
Regime 1:					
σ^2, diversification rate	3.18 ± .08	443.51 ± 53.24	165.39 ± 70.80	420.21 ± 31.13	72.42 ± 4.46
α, restoring force	NA	12.49 ± .21	3.14 ± .25	24.67 ± .71	NA
θ, optimum (OU) or ancestral mean (BM)	51.45 ± 1.52	52.60 ± 1.74	55.13 ± 1.92	52.92 ± .98	52.24 ± 7.14
Regime 2:					
σ^2, diversification rate	110.81 ± 6.43	443.51 ± 53.24	165.39 ± 70.80	1,796.62 ± 5,531.86	72.42 ± 4.46
α, restoring force	NA	12.49 ± .21	3.14 ± .25	24.67 ± .71	NA
θ, optimum (OU) or ancestral mean (BM)	51.45 ± 1.52	59.29 ± 1.19	55.13 ± 1.92	59.17 ± 1.20	52.24 ± 7.14

Note: Change in Akaike information criterion corrected for sample size (ΔAICc), relative to model BMS, is shown in the first row. Calculation of standard errors, provided after each plus-or-minus sign, is described in the text.

parameter ω_{zii} by setting $G_{ii} = 0.4$, a modal value for morphological traits (Estes and Arnold 2007), and realizing that $t = 200{,}000$ generations. We find that ω_{zii} is approximately 6,404 (table 2). Although this estimate of stabilizing selection is based on ornament data, recall from our simulations of the FLP that ornament evolution is governed by natural selection on preferences and, indeed, that ornament diversification mirrors preference diversification (fig. 6). These considerations suggest that 6,404 might be taken as a rough approximation of the magnitude of stabilizing selection acting on preferences (ω_{yii}). By this logic, the other OU models yield estimates of ω_{yii} that are either stronger (3,242) or weaker (25,477).

From figure 6, we can derive a useful approximation from the fact that the 95% confidence limits for ornament diversification (red dotted lines) are approximated by two times the 99% confidence limits for diversification in preference by natural selection alone (red solid line). Let V_y be the empirically observed variance in preference means under a FLP model that includes natural and sexual selection. Then our statement about equivalence of confidence limits becomes

$$1.96\sqrt{V_y} \approx 2(2.576)\sqrt{\frac{\omega_{yii} + Q}{N_e}}, \tag{5a}$$

where the expression in the square root sign on the right is the limiting value for variance in preference means under natural selection alone (1). Fitting OU models with OUwie provides an estimate of the diversification rate σ^2, which is equivalent to variance in ornament means and hence to V_y. Rearranging the above expression and solving for stabilizing selection on preferences, we have

$$\omega_{yii} \approx \frac{N_e\sigma^2}{1.341} - 1. \tag{5b}$$

Using this expression to estimate the magnitude of stabilizing selection with values of N_e ranging from 5,000 to 50,000 and estimates of σ^2 from OUwie models OUM, OU1, and OUMV, we obtain the values of ω_{zii} and, hence, ω_{yii} ranging from 10^5 to 10^7 (table 2). In other words, the restoring force of natural selection on preferences is apparently extremely weak, regardless of which model is used to estimate it.

Under the genetic drift interpretation of BM, the estimated diversification rate σ^2 is equivalent to $G_{ii}t/N_e$. Using the values for G_{ii} and t shown in table 4, we obtain estimates of effective population size of 25,157 in regime 1 and 722 in regime 2 using the BMS model. To put these numbers in perspective, in a sample of eight noncolonial bird species, N_e estimates ranged from 176 to 7,678, with an average of 1,993 (Barrowclough 1980). Clearly, BMS is struggling to account for the modest, slower differentiation in regime 1 with a value for N_e that seems unrealistically large and for the more substantial, faster differentiation in regime 2 with an unrealistically small N_e. Likewise, BM1, which fits a single value of σ^2, estimates N_e as 1,105, which seems plausible on the basis of Barrowclough's (1980) survey but is probably unrealistically small on a 10^5-generation timescale. We conclude from this exercise that we can reject the genetic drift interpretation of BM because the estimated values of N_e are unrealistic.

Under the adaptive peak movement interpretation of BM, we can estimate the per generation rate of peak movement. OUwie diversification rate σ^2 is equivalent to $t\sigma^2_\theta$, providing three estimates of σ^2_θ (table 4). Using the fastest of these rates ($\sigma^2_\theta = 0.00055$, for regime 2 using BMS) for the movement of natural selection optimum for preference, we can easily account for a birds of paradise–comparable radiation in wing length in as few as 20,000 generations (fig. 7).

Table 4: Estimates of Fisher-Lande process parameters from OUwie parameter estimates

	Regime	G_{ii}	P_{ii}	t	α	ω_{zii}
OU models:						
Estimates of stabilizing selection from OUwie parameter α:						
OUM	NA	.4	1	200,000	12.49	6,404
OU1	NA	.4	1	200,000	3.14	25,477
OUMV	NA	.4	1	200,000	24.67	3,242
	Regime	N_e	P_{ii}	σ^2		ω_{zii}
Estimates of stabilizing selection from OUwie parameter σ^2:						
OUM	NA	5,000	1	443.51	. . .	1,653,653
OUM	NA	50,000	1	443.51	. . .	16,536,539
OU1	NA	5,000	1	165.39	. . .	616,666
OU1	NA	50,000	1	165.39	. . .	6,166,666
OUMV	1	5,000	1	420.21	. . .	1,566,778
OUMV	1	50,000	1	420.21	. . .	15,667,784
OUMV	2	5,000	1	1,796.62	. . .	6,698,806
OUMV	2	50,000	1	1,796.62	. . .	66,988,068
	Regime	G_{ii}	t	σ^2		N_e
BM models:						
Estimates of effective population size from OUwie parameter σ^2:						
BMS	1	.4	200,000	3.18	. . .	25,157
BMS	2	.4	200,000	110.81	. . .	722
BM1	NA	.4	200,000	72.42	. . .	1,105
	Regime		t	σ^2		σ^2_θ
Estimates of the rate of peak movement from OUwie parameter σ^2:						
BMS	1	. . .	200,000	3.18	. . .	.0000159
BMS	2	. . .	200,000	110.81	. . .	.0005541
BM1	NA	. . .	200,000	72.41	. . .	.0003621

Note: BM = Brownian motion; OU = Ornstein-Uhlenbeck.

That result suggests that peak movement is a more plausible model of BM than genetic drift.

Discussion

Qualitative Insights from the Phenotypic Tango Model

Our focus on the factors that determine the size and shape of sexual radiations fundamentally reorders long-standing perspectives on the FLP. Focusing first on drift-selection balance results, we find that natural selection on preferences controls the sexual radiation in ornaments. In particular, the strength and pattern of stabilizing selection on preferences defines the evolutionary trait space (dance floor) within which ornaments achieve a stable balance between drift and selection. Second, effective population size is the other major factor defining the dance floor. In contrast, natural selection on ornaments has relatively little effect on the diversification of ornaments because even with a modest strength of mate choice (moderately small ν), evolving preferences pull ornaments into a stable equilibrium cloud that extends far from their optimum. Inheritance plays an even smaller role in defining the boundaries of ornament diversification in the sense that a genetic correlation between the sexes can amplify the diversification of both preferences and ornaments, but the amplification may not be large. Alternatively, if we try to account for sexual radiations with moving preference optimum, we find that the rate at which that optimum moves completely dominates the extent of the sexual radiation, overshadowing the effects of all other parameters.

Stepping back from the specifics of our analysis, one aspect of the overview is surprising. With the addition of selection on preferences, Lande's (1981) model becomes an OU model in which diversification is bounded instead of perpetually expanding by drift (Uyeda et al. 2009), but be-

cause evolution is bounded the crucial features of the model are parameters that define boundaries rather than those that define evolutionary rates. This contrast is vividly illuminated by the bird of paradise case study because we find that we have plenty of time for the radiation to emerge. The big puzzle is how the radiation is shaped and constrained. Those are issues not of rate but of constraint.

Quantitative Insights from the Phenotypic Tango Model

We found that we must invoke either extremely weak natural selection on preferences or allow the preference optimum to move to account for the quantitative aspects of ornament diversification in birds of paradise. We reached this conclusion by placing particular parameters within realistic bounds (e.g., heritability, genetic correlation, N_e, and selection on ornaments) and asking what values of other key parameters were required to account for the radiation of ornaments. In the case of a stationary preference optimum, we found that stabilizing selection on preferences needs to be four orders of magnitude weaker than stabilizing selection on ornaments and that effective population size must be relatively small ($N_e = 500$; fig. 6). We can determine what other parameter combinations will give equivalent results by noting that the limiting width of the ornament radiation will be proportional to $(\omega_{yii} + 1)/2N_e$ (see expression [1]). In figure 6, this expected variance was $10^4/10^3 = 10$, so we can anticipate radiations of comparable size when $\omega_{yii} + 1$ is 10^5 and N_e is 50,000 (or $\omega_{yii} + 1 = 10^6$ and $N_e = 500{,}000$). In any of these cases, we are invoking stabilizing selection much weaker than that which can be measured in nature. One might be tempted to conclude that such selection is so weak that we might as well conclude that preferences are selectively neutral. This argument overlooks the important effect that even extremely weak stabilizing selection can have on a timescale of a million generations or more. On such a long timescale, the weak selection that we invoke puts stable limits on diversification that stop ornaments from evolving to truly absurd sizes.

Alternatively, we can account for ornament radiations comparable to *Paradisaea* with a FLP in which the preference optimum moves by BM. The rate of random motion that we used in figure 7 was about 2% of a within-population phenotypic standard deviation in preference each generation, which seems remarkably modest given the magnitude of radiation in ornaments that it can produce in a few tens of thousands of generations. The other remarkable feature of this model is that the long-term magnitude of the radiation is a function of elapsed time and the rate of peak movement and not a function of other parameters of selection or inheritance.

Quantitative Insights from the Generic OU and BM Models

The major conclusion emerging from our analysis using OUwie is that a modest rate of peak movement could account for the ornament diversification that we observe in one bird of paradise genus. If we imagine that the natural selection optimum for preferences moves randomly at a rate in the range of only 0.4%–2% of a phenotypic standard deviation per generation, we obtain our best fits to data on ornament diversification. In contrast, other interpretations of the best-fitting generic models are much less palatable. For example, if we use the genetic drift interpretation of the best-fitting BM model (BMS), we must imagine that N_e changes from about 25,000 in one section of the phylogeny to about 700 in another section. Alternatively, if we chose one of the best-fitting OU models, we must invoke the same extraordinarily weak selection on preferences that gave us pause using the phenotypic tango model (i.e., $\omega_{yii} + 1 = 10^5$ to 10^7). These considerations lead to the conclusion that peak movement (by BM or some other process) is the key to understanding extraordinary evolution of preferences and, hence, of ornaments. The point that peak movement will probably be a necessary ingredient for successful modeling of adaptive radiations has been made in a broader context (Arnold et al. 2002; Estes and Arnold 2007; Hansen et al. 2008; Uyeda et al. 2011; Beaulieu et al. 2012). In general, successful models need to balance factors promoting stasis (e.g., stabilizing selection) with factors that promote diversification (e.g., drift, peak movement). This need for pairing suggests that if we try to explain sexual radiations using more complicated models of preference evolution (e.g., including handicaps, indicator traits, or sexual conflict), we will need to compensate for the constraints that those elaborations impose with diversification amplifiers such as peak movement.

Birds of Paradise and Beyond

Despite success in finding an explanation for some aspects of the plumage radiation in one genus of birds of paradise, we have not attempted to explain other aspects of that and other sexual radiations. For example, sexual radiations are often characterized by bursts of unusual ornament evolution that are restricted to one or a few lineages in a clade. The elongate white wrist plumes unique to the standard-wing bird of paradise (*Semioptera wallacii*) or the unusual head plumes of the king of Saxony bird of paradise (*Pteridophora alberti*) are examples. Although the versions of the FLP that we have explored do little to illuminate the origin of these kinds of novelties, we might be able to account for them with a modest extension of the moving optimum feature. One could define thresholds on the trait scales such

that the trait (ornament or preference) is expressed once trait mean evolves beyond the threshold (Wright 1934; Felsenstein 2012). Expression could mean that the ornament becomes detectable by the sensory systems of the female or that the preference now plays a role in mate choice. By this modeling device one might account for the rapid origin of new ornaments or for the loss of old ones. The broader point is that the multivariate version of the FLP described here could be extended to explain many otherwise enigmatic features of sexual radiation.

The methods that we have used to resolve evolutionary process and estimate its parameters in birds of paradise could be easily applied to other sexual radiations. The essential ingredients are measurements of sexually selected traits in multiple taxa with a time-calibrated phylogeny. Although we used a data set with only 14 taxa, simulations by Beaulieu et al. (2012) indicate that dozens or scores of taxa will often be needed to get accurate parameter estimates with OUwie. Aside from advocating the use of larger data sets that we employed here, we also recommend making continuous measurements of traits rather than using a small number of trait categories. Continuous traits give access to the most powerful models of evolutionary process.

Conclusions

The confrontation that we have described between data and theory reveals both empirical and theoretical issues. On the empirical side, we see a general need for more quantitative data that describe both the scope and the time course of evolution driven by sexual selection. In the case of birds of paradise, we need data from more species and populations, with measurements focused on the acoustic and behavioral as well as the morphological components of male display. On the theoretical side, the growing ability to test alternative models with tree-based data is certainly an important path forward (Arnold 2014). But for all their strengths, the available models and testing frameworks suffer from some conspicuous limitations. In the bird of paradise test case, we showed that a model of peak movement by BM provided the best fit to our data, and we were able to estimate the parameter of peak movement by maximum likelihood. This success, however, leaves us stranded short of illuminating the details of bird of paradise population and behavioral biology. In this article, we bridged that gap using the phenotypic tango model of the FLP and gained additional perspective on the processes driving the bird of paradise radiation. One promising avenue forward will be to use testing frameworks that incorporate quantitative prior information about selection, inheritance, and population size. Such a framework has been described and implemented by Uyeda and Harmon (2014). Beyond those improvements, we also need to embed the FLP in a testing framework that addresses the essential complexities of sexual radiation. In particular, these radiations ramify in multivariate phenotypic space. Consequently, we need to test quantitative genetic FLP models that reflect the reality that female choice is based on multiple, interacting male traits that broadcast in multiple sensory modalities (Heisler 1985; Pomiankowksi and Iwasa 1993; Iwasa and Pomiankowski 1994). An additional goal should be to see if lessons emerging from population genetic modeling of the FLP (van Doorn and Weissing 2004, 2006) will hold in quantitative genetic models and help explain sexual radiations. In general, we need to test multivariate models that capture the essence of sexual communication. The phenotypic tango model is a step in this direction, but only a step.

Acknowledgments

We are grateful to J. Beaulieu, J. Cracraft, R. Feldhoff, M. Feldman, J. Felsenstein, H. Godwin, T. Hansen, B. O'Meara, W. Swanson, R. Watts, D. Wilburn, two anonymous reviewers, and participants in the NIMBioS 2015 tutorial in evolutionary quantitative genetics for helpful discussions and comments. Thanks to I. Phillipsen for artwork. This work was supported by National Science Foundation (NSF) grant DEB-0947162 to S.J.A. and NSF grant IOS-0818554 to L.D.H.

APPENDIX A

Details of the Phenotypic Tango Model

The following results are derived from results in Lande (1981) unless noted otherwise. The model is presented for multiple ornaments and preferences but is illustrated for just the bivariate case (matrices and vectors are denoted with boldface). The phenotypic values of two male ornament traits $\boldsymbol{z} = (z_1, z_2)^{\mathrm{T}}$, where T denotes transpose, and two female preference traits $\boldsymbol{y} = (y_1, y_2)^{\mathrm{T}}$ are each affected by multiple genes and environmental effects. The phenotypic values of the four traits are multivariate normally distributed and genetically uncorrelated within a sex before selection with means denoted by column vectors, $\bar{\boldsymbol{z}}$ and $\bar{\boldsymbol{y}}$, and with variance-covariance matrices, which are 2×2 in the bivariate case, denoted by **P** and **Q**, respectively. The corresponding inheritance matrices for the traits are the 2×2 symmetric matrices **G** and **H**, with additive genetic variances on their diagonals and additive genetic covariances elsewhere. A third 2×2 symmetric matrix, **B**, describes genetic covariances between the sexes.

The deterministic responses of the trait means to selection from one generation to the next are a function of additive genetic variance/covariance and the selection gradients

$$\begin{bmatrix} \Delta\bar{\boldsymbol{z}} \\ \Delta\bar{\boldsymbol{y}} \end{bmatrix} = \begin{bmatrix} \Delta\bar{z}_1 \\ \Delta\bar{z}_2 \\ \Delta\bar{y}_1 \\ \Delta\bar{y}_2 \end{bmatrix} = \tfrac{1}{2}\begin{bmatrix} \mathbf{G} & \mathbf{B} \\ \mathbf{B} & \mathbf{H} \end{bmatrix}\begin{bmatrix} \boldsymbol{\beta}_z \\ \boldsymbol{\beta}_y \end{bmatrix}, \tag{A1}$$

where the factor of ½ accounts for sex-limited trait expression and $\boldsymbol{\beta}_z$ and $\boldsymbol{\beta}_y$ are, respectively, the selection gradients for ornaments and preferences (see Lande 1980*b*, 1981). The additive genetic variance/covariance matrix for the trait vector $(z, y)^{\mathrm{T}}$ takes the following form:

$$\tfrac{1}{2}\begin{bmatrix} \mathbf{G} & \mathbf{B} \\ \mathbf{B} & \mathbf{H} \end{bmatrix} = \tfrac{1}{2}\begin{bmatrix} G_{11} & G_{12} & B_{11} & B_{12} \\ G_{12} & G_{22} & B_{12} & B_{22} \\ B_{11} & B_{12} & H_{11} & H_{12} \\ B_{12} & B_{22} & H_{12} & H_{22} \end{bmatrix}. \tag{A2}$$

Stabilizing natural selection acts on the ornaments. The individual selection function describing this selection is Gaussian in shape with an optimum at $\boldsymbol{\theta}_z = (\theta_{z1}, \theta_{z2})^{\mathrm{T}}$ and width parameters

$$\boldsymbol{\omega}_z = \begin{bmatrix} \omega_{z11} & \omega_{z12} \\ \omega_{z12} & \omega_{z22} \end{bmatrix},$$

with elements analogous to variances and covariances. In other words, the expected fitness of an individual male with trait values z_1 and z_2 is

$$W(z) = \exp\{-\tfrac{1}{2}(\boldsymbol{z} - \boldsymbol{\theta}_z)^{\mathrm{T}}\boldsymbol{\omega}_z^{-1}(\boldsymbol{z} - \boldsymbol{\theta}_z)\} \tag{A3}$$

(Lande 1979, 1980*b*). This natural selection shifts the mean of the trait from $\bar{\boldsymbol{z}} = (\bar{z}_1, \bar{z}_2)^{\mathrm{T}}$ to $\bar{\mathbf{z}}^* = (\bar{z}_1^*, \bar{z}_2^*)^{\mathrm{T}}$, so that after natural selection the ornaments are multivariate normally distributed with mean and variance-covariance given by

$$\bar{\mathbf{z}}^* = (\boldsymbol{\omega}_z + \mathbf{P})^{-1}(\boldsymbol{\omega}_z\bar{\boldsymbol{z}} + \mathbf{P}\boldsymbol{\theta}_z), \tag{A4a}$$

$$\mathbf{P}^* = (\boldsymbol{\omega}_z^{-1} + \mathbf{P}^{-1})^{-1} = \mathbf{P} - \mathbf{P}(\boldsymbol{\omega}_z + \mathbf{P})^{-1}\mathbf{P} \tag{A4b}$$

(Lande 1980*a*). Consequently, the shifts in the means of the ornaments—their natural selection differentials—are

$$\boldsymbol{s}_{zns} = \bar{\boldsymbol{z}}^* - \bar{\boldsymbol{z}} = \begin{bmatrix} \bar{z}_1^* - \bar{z}_1 \\ \bar{z}_2^* - \bar{z}_2 \end{bmatrix} = (\boldsymbol{\omega}_z + \mathbf{P})^{-1}\mathbf{P}(\boldsymbol{\theta}_z - \bar{\boldsymbol{z}}). \tag{A5}$$

Analogous natural selection acts on the female preference traits. As with the ornaments, we assume that directional and stabilizing natural selection acts on the preferences. Letting this natural selection be Gaussian in form with an optimum at $\boldsymbol{\theta}_y = (\theta_{y1}, \theta_{y2})^{\mathrm{T}}$ and width parameters

$$\boldsymbol{\omega}_y = \begin{bmatrix} \omega_{y11} & \omega_{y12} \\ \omega_{y12} & \omega_{y22} \end{bmatrix},$$

we obtain the following expression for the relative fitness of a female with preference traits values $\boldsymbol{y}$:

$$W(y) = \exp\{-\tfrac{1}{2}(\boldsymbol{y} - \boldsymbol{\theta}_y)^{\mathrm{T}}\boldsymbol{\omega}_y^{-1}(\boldsymbol{y} - \boldsymbol{\theta}_y)\}. \tag{A6}$$

The preference means and variances after natural selection are

$$\bar{\boldsymbol{y}}^* = (\boldsymbol{\omega}_y + \mathbf{Q})^{-1}(\boldsymbol{\omega}_y\bar{\boldsymbol{y}} + \mathbf{Q}\boldsymbol{\theta}_y), \tag{A7a}$$

$$\mathbf{Q}^* = (\boldsymbol{\omega}_y^{-1} + \mathbf{Q}^{-1})^{-1} = \mathbf{Q} - \mathbf{Q}(\boldsymbol{\omega}_y + \mathbf{Q})^{-1}\mathbf{Q}, \tag{A7b}$$

giving the selection differentials

$$\boldsymbol{S}_y = \bar{\boldsymbol{y}}^* - \bar{\boldsymbol{y}} = \begin{bmatrix} \bar{y}_1^* - \bar{y}_1 \\ \bar{y}_2^* - \bar{y}_2 \end{bmatrix} = (\boldsymbol{\omega}_y + \mathbf{Q})^{-1}\mathbf{Q}(\boldsymbol{\theta}_y - \bar{\boldsymbol{y}}) \tag{A8a}$$

and the selection gradients

$$\boldsymbol{\beta}_y = \mathbf{Q}^{-1}\boldsymbol{S}_y = (\boldsymbol{\omega}_y + \mathbf{Q})^{-1}(\boldsymbol{\theta}_y - \bar{\boldsymbol{y}}) \tag{A8b}$$

for the preference traits.

Female mate choice exerts sexual selection on the distributions of ornaments after natural selection, causing additional shifts in the ornament means. The tendency of a particular female with preference value $\boldsymbol{y}$ to mate with a particular male with ornament value $\boldsymbol{z}$ is proportional to a multivariate Gaussian function $\psi(\boldsymbol{z}|\boldsymbol{y})$ with an optimum at $\boldsymbol{y}$ and width parameters

$$\boldsymbol{\nu} = \begin{bmatrix} \nu_{11} & \nu_{12} \\ \nu_{12} & \nu_{22} \end{bmatrix},$$

as follows:

$$\psi(\boldsymbol{z}|\boldsymbol{y}) = \begin{bmatrix} \psi(z_1|y_1) \\ \psi(z_2|y_2) \end{bmatrix} \propto \exp\{-\tfrac{1}{2}(\boldsymbol{z} - \boldsymbol{y})^{\mathrm{T}}\boldsymbol{\nu}^{-1}(\boldsymbol{z} - \boldsymbol{\theta}_z)\}. \tag{A9}$$

Averaging these functions over the ornament trait distributions after natural selection, we find that the average ornament traits of the males that mate with a female with preference value y deviate from her personal optimum by amounts given by

$$(\boldsymbol{\nu} + \mathbf{P}^*)^{-1}\mathbf{P}^*(\boldsymbol{y} - \bar{\boldsymbol{z}}^*). \tag{A10}$$

Averaging over the female preference distribution after natural selection, we find that the average tendency of females to mate with a male with ornament value z is a Gaussian function:

$$\psi(\boldsymbol{z}) = \begin{bmatrix} \psi(z_1) \\ \psi(z_2) \end{bmatrix} \propto \exp\{-\tfrac{1}{2}(\boldsymbol{z} - \bar{\boldsymbol{y}}^*)^{\mathrm{T}}(\mathbf{Q}^* + \boldsymbol{\nu})^{-1}(\boldsymbol{z} - \bar{\boldsymbol{y}}^*)\} \tag{A11}$$

(Arnold et al. 1996, expression [4]). These expressions allow us to solve for the shift in the ornament means caused by sexual selection:

$$\mathbf{S}_{zss} = (\boldsymbol{\nu} + \mathbf{P}^*)^{-1}\mathbf{P}^*(\bar{\boldsymbol{y}}^* - \bar{\boldsymbol{z}}^*) = (\boldsymbol{\nu} + \mathbf{P}^*)^{-1}\mathbf{P}^*\begin{bmatrix}\bar{y}_1^* - \bar{z}_1^* \\ \bar{y}_2^* - \bar{z}_2^*\end{bmatrix}. \tag{A12}$$

Combining this sexual selection differential with the natural selection differential, we obtain the total selection differential and gradients for the ornaments (Lande 1980*b*):

$$\mathbf{S}_z = \mathbf{S}_{zns} + \mathbf{S}_{zss}, \tag{A13a}$$

$$\boldsymbol{\beta}_z = \mathbf{P}^{-1}\mathbf{S}_z = (\boldsymbol{\omega}_z + \mathbf{P})^{-1}(\boldsymbol{\theta}_z - \bar{\boldsymbol{z}}) + \mathbf{P}^{-1}(\boldsymbol{\nu} + \mathbf{P}^*)^{-1}\mathbf{P}^*(\bar{\boldsymbol{y}}^* - \bar{\boldsymbol{z}}^*). \tag{A13b}$$

We used this exact expression in our simulations. If, following Lande (1981), we let preferences and natural selection be weak so that $\boldsymbol{\omega}_z, \boldsymbol{\nu} \gg \mathbf{P}$, the above expression yields his approximation for the total net selection gradient acting on a single ornament:

$$\beta_z = P^{-1}S_z \approx {\omega_z}^{-1}\left\{\frac{\bar{y}^*}{\alpha_{ii}} - \left(1 + \frac{1}{\alpha_{ii}}\right)\bar{z} + \theta_z\right\}, \tag{A14}$$

where

$$\boldsymbol{\alpha} = \begin{bmatrix}\alpha_{11} & \alpha_{12} \\ \alpha_{12} & \alpha_{22}\end{bmatrix} = \boldsymbol{\omega}_z^{-1}\boldsymbol{\nu}$$

and $\alpha_{ii} = \alpha_{11} = \alpha_{22}$.

We can solve for the equilibrium of the deterministic process by setting our expressions for selection gradients ([A8b] and [A13b]) equal to 0 and solving for the values of the preference and ornament means. The resulting expression for equilibrium preference mean is simple,

$$\hat{\boldsymbol{y}} = \boldsymbol{\theta}_y, \tag{A15a}$$

but the expression for the equilibrium ornament mean is more complicated. Simplifying that expression by assuming that $\boldsymbol{\omega}_z, \boldsymbol{\nu} \gg \mathbf{P}$, we obtain an expression for the ornament mean at equilibrium:

$$\begin{aligned}\hat{\boldsymbol{z}} &\approx \boldsymbol{\omega}_z^{-1}(\boldsymbol{\theta}_z - \bar{\boldsymbol{z}}) + \boldsymbol{\nu}^{-1}(\bar{\boldsymbol{y}}^* - \bar{\boldsymbol{z}}^*) \\ &\approx (\boldsymbol{\omega}_z^{-1} + \boldsymbol{\nu}^{-1})^{-1}(\boldsymbol{\omega}_z^{-1} - \boldsymbol{\nu}^{-1}\boldsymbol{\omega}_z^{-1}\mathbf{P})\boldsymbol{\theta}_z + (\boldsymbol{\omega}_z^{-1} + \boldsymbol{\nu}^{-1})^{-1}\boldsymbol{\nu}^{-1}\boldsymbol{\theta}_y.\end{aligned} \tag{A15b}$$

The first expression on the right is not a closed solution because $\bar{\boldsymbol{z}}$ occurs in both of its terms, but it makes the equilibrium condition transparent by showing how the balance between natural and sexual selection arises. The final expression is a closed solution, but it is considerably less transparent. In other words, at equilibrium the preference mean is at its optimum, but the ornament mean may strongly deviate from its natural selection optimum in the direction of the preference optimum.

Substituting expressions (A8b) and (A13b) for the two selection gradients into expression (A1), we obtain our equations for the response of the ornament and preference means to the combined forces of natural and sexual selection. In our simulations, the expressions for selection response took a simple form because we assumed that traits were genetically uncorrelated within each sex. Furthermore, to simplify implementation of the model, we generally assumed that the additive genetic variance/covariance matrix for the trait vector $(\boldsymbol{z}, \boldsymbol{y})^{\mathrm{T}}$ took the following form:

$$\tfrac{1}{2}\begin{bmatrix}\mathbf{G} & \mathbf{B} \\ \mathbf{B} & \mathbf{H}\end{bmatrix} = \tfrac{1}{2}\begin{bmatrix}G_{11} & 0 & B_{11} & 0 \\ 0 & G_{22} & 0 & B_{22} \\ B_{11} & 0 & H_{11} & 0 \\ 0 & B_{22} & 0 & H_{22}\end{bmatrix}. \tag{A16}$$

In our simulations, we used the following expression for the stochastic evolution of ornaments and preferences:

$$\begin{bmatrix}\Delta\bar{\boldsymbol{z}} \\ \Delta\bar{\boldsymbol{y}}\end{bmatrix} = \begin{bmatrix}\Delta\bar{z}_1 \\ \Delta\bar{z}_2 \\ \Delta\bar{y}_1 \\ \Delta\bar{y}_2\end{bmatrix} = \tfrac{1}{2}\begin{bmatrix}\mathbf{G} & \mathbf{B} \\ \mathbf{B} & \mathbf{H}\end{bmatrix}\begin{bmatrix}\boldsymbol{\beta}_z \\ \boldsymbol{\beta}_y\end{bmatrix} + N\left[0, \frac{1}{2N_e}\begin{bmatrix}\mathbf{G} & \mathbf{B} \\ \mathbf{B} & \mathbf{H}\end{bmatrix}\right] \tag{A17}$$

(Lande 1979, 1980*b*). The first term on the right involves direct responses to selection as well as correlated responses to selection such that selection on a preference trait evokes a response in a genetically correlated ornament trait and vice versa. The last term on the right specifies changes in trait means due to genetic drift (Lande 1979). In other words,

$$N\left[0, \frac{\begin{bmatrix}\mathbf{G} & \mathbf{B} \\ \mathbf{B} & \mathbf{H}\end{bmatrix}}{2N_e}\right]$$

denotes a draw of a vector of change in four values, $(z_1, z_2, y_1, y_2)^{\mathrm{T}}$, from a multivariate normal distribution with a mean vector of zeros and a variance-covariance matrix of

$$\frac{\begin{bmatrix}\mathbf{G} & \mathbf{B} \\ \mathbf{B} & \mathbf{H}\end{bmatrix}}{2N_e},$$

where N_e is effective population size.

In the absence of sexual selection, the genetic correlation between the sexes is not maintained, $B_{11} = B_{22} = 0$, and the expression for per generation evolution simplifies further to

$$\begin{bmatrix}\Delta\bar{\boldsymbol{z}} \\ \Delta\bar{\boldsymbol{y}}\end{bmatrix} = \begin{bmatrix}\Delta\bar{z}_1 \\ \Delta\bar{z}_2 \\ \Delta\bar{y}_1 \\ \Delta\bar{y}_2\end{bmatrix} = \begin{bmatrix}\tfrac{1}{2}G_{11}\beta_{z1} \\ \tfrac{1}{2}G_{22}\beta_{z2} \\ \tfrac{1}{2}H_{11}\beta_{y1} \\ \tfrac{1}{2}H_{22}\beta_{y2}\end{bmatrix} + \begin{bmatrix}N(0, G_{11}/2N_e) \\ N(0, G_{22}/2N_e) \\ N(0, H_{11}/2N_e) \\ N(0, H_{22}/2N_e)\end{bmatrix}, \tag{A18}$$

where

$$\begin{bmatrix} \beta_{z1} \\ \beta_{z2} \end{bmatrix} = \begin{bmatrix} S_{z1}/P_{11} \\ S_{z2}/P_{22} \end{bmatrix} \tag{A19a}$$

and

$$\begin{bmatrix} \mathbf{S}_{z1} \\ \mathbf{S}_{z2} \end{bmatrix} = \begin{bmatrix} \bar{z}_1^* - \bar{z}_1 \\ \bar{z}_2^* - \bar{z}_2 \end{bmatrix} = \begin{bmatrix} \dfrac{\omega_{z11}\bar{z}_1 + P_{11}\theta_{z1}}{\omega_{z11} + P_{11}} - \bar{z}_1 \\ \dfrac{\omega_{z22}\bar{z}_2 + P_{22}\theta_{z2}}{\omega_{z22} + P_{22}} - \bar{z}_2 \end{bmatrix}, \tag{A19b}$$

and similarly for the selection differentials and gradients on preferences. In these expressions, we have also assumed that there is no genetic covariance within the sexes and that the off-diagonal terms in $\boldsymbol{\omega}_z$ and $\boldsymbol{\omega}_y$ are 0.

We can also specify the distribution of trait means in a set of replicate populations evolving by natural selection alone. Because all traits evolve independently in the absence of sexual selection, we can apply Lande's (1976*b*) results for a single trait evolving toward stabilizing selection-drift balance in multiple replicate lineages. Setting the trait optima at 0, after t generations the means of the ornaments of the replicate lineages will be multivariate normally distributed with means of 0 and variance-covariance given by

$$\mathrm{Var}[\bar{\boldsymbol{z}}(t)] = \frac{\boldsymbol{\omega}_z + \mathbf{P}}{2N_e}\{1 - \exp[-2((\boldsymbol{\omega}_z + \mathbf{P})^{-1}\mathbf{G})t]\}. \tag{A20}$$

Even when stabilizing natural selection is relatively weak, the distribution of trait means rapidly reaches a long-term equilibrium variance-covariance given by $(\boldsymbol{\omega}_z + \mathbf{P})/N_e$. An analogous expression holds for the stochastic evolution of preferences under natural selection alone.

If the natural selection optimum moves by BM, we can solve expressions that summarize the dynamics of the process, but the variance expression is more complicated than expression (A20) (Hansen et al. 2008). In particular, in the case of genetically and phenotypically uncorrelated ornaments, the distribution of lineage means at generation t is normal, with a mean given by the common position of the optimum at generation 0 and with variance given by the following univariate expression:

$$\begin{aligned} \mathrm{Var}[\bar{z}(t)] = {} & \frac{\sigma_\theta^2 + (G/N_e)}{2a}\{1 - \exp[-2at]\} \\ & + \sigma_\theta^2 t\left\{1 - 2\frac{(1 - \exp[-at])}{at}\right\}, \end{aligned} \tag{A21a}$$

where $a = (\omega_z + P)^{-1}G$ and σ_θ^2 is the variance in the position of the optimum, θ. This expression rapidly converges to

$$\mathrm{Var}[\bar{z}(t)] = t\sigma_\theta^2. \tag{A21b}$$

In other words, the details of inheritance and selection (other than the movement of the optimum) have no effect on the long-term pattern of the adaptive radiation.

Literature Cited

Arnold, S. J. 1983. Sexual selection: the interface of theory and empiricism. Pages 67–107 *in* P. P. G. Bateson, ed. Mate choice. Cambridge University Press, Cambridge.

———. 1985. Quantitative genetic models of sexual selection. Experientia 41:1296–1310.

———. 2014. Phenotypic evolution: the ongoing synthesis. American Naturalist 183:729–746.

Arnold, S. J., and L. D. Houck. 2016. Data from: Can the Fisher-Lande process account for birds of paradise and other sexual radiations? American Naturalist, Dryad Digital Repository, http://dx.doi.org/10.5061/dryad.66ft5.2.

Arnold, S. J., M. E. Pfrender, and A. G. Jones. 2002. The adaptive landscape as a conceptual bridge between micro- and macroevolution. Pages 9–32 *in* A. P. Hendry and M. T. Kinnison, eds. Microevolution rate, pattern, process. Kluwer, Dordrecht.

Arnold, S. J., P. A. Verrell, and S. G. Tilley. 1996. The evolution of asymmetric sexual isolation: a polygenic model and a test case. Evolution 50:1024–1033.

Barrowclough, G. F. 1980. Gene flow, effective population sizes, and genetic variance components in birds. Evolution 34:789–798.

Beaulieu, J. M., D.-C. Jhwueng, C. Boettiger, and B. C. O'Meara. 2012. Modeling stabilizing selection: expanding the Ornstein-Uhlenbeck model of adaptive evolution. Evolution 66:2369–2383.

Bürger, R., and R. Lande. 1994. On the distribution of the mean and variance of a quantitative trait under mutation-selection-drift balance. Genetics 138:901–912.

Danchin, É., L.-A. Giraldeau, and F. Cézilly. 2008. Behavioural ecology. Oxford University Press, Oxford.

Day, T. 2000. Sexual selection and the evolution of costly female preferences: spatial effects. Evolution 54:715–730.

Dinsmore, J. T. 1970. Courtship behavior of the greater bird of paradise. Auk 87:305–321.

Estes, S., and S. J. Arnold. 2007. Resolving the paradox of stasis: models with stabilizing selection explain evolutionary divergence on all timescales. American Naturalist 169:227–244.

Felsenstein, J. 1985. Phylogenies and the comparative method. American Naturalist 125:1–15.

———. 2012. A comparative method for both discrete and continuous characters using the threshold model. American Naturalist 179:145–156.

Firth, C. B. 1976. Displays of the red bird-of-paradise *Paradisaea rubra* and their significance, with a discussion on displays and systematics of other Paradisaeidae. Emu 76:69–78.

Fisher, R. A. 1915. The evolution of sexual preference. Eugenics Review 7:184–192.

———. (1930) 1958. The genetical theory of natural selection. 2nd ed. Dover, New York. Original edition, Clarendon, London.

Grace, J. L., and K. L. Shaw. 2011. Coevolution of male mating signal and female mating preference during the early lineage divergence of the Hawaiian cricket, *Laupala cerasina*. Evolution 65:2184–2196.

Grafen, A. 1990. Sexual selection unhandicapped by the Fisher process. Journal of theoretical Biology 144:473–516.

Hansen, T. F. 1997. Stabilizing selection and the comparative analysis of adaptation. Evolution 51:1341–1351.

Hansen, T. F., J. Pienaar, and S. H. Orzack. 2008. A comparative method for studying adaptation to a randomly evolving environment. Evolution 62:1965–1977.

Heisler, I. L. 1985. Quantitative genetic models of female choice based on "arbitrary" male characters. Heredity 55:187–198.

Hoglund, J., and R. V. Alatalo. 2014. Leks. Princeton University Press, Princeton, NJ.

Irestedt, M., K. A. Jønsson, J. Fjeldså, L. Christidis, and P. G. P. Ericson. 2009. An unexpectedly long history of sexual selection in birds-of-paradise. BMC Evolutionary Biology 9:235.

Iwasa, Y., and A. Pomiankowski. 1994. The evolution of mate preferences for multiple ornaments. Evolution 48:853–867.

———. 1995. Continual change in mate preferences. Nature 377: 420–422.

Jones, A. G., S. J. Arnold, and R. Bürger. 2003. Stability of the **G**-matrix in a population experiencing mutation, stabilizing selection, and genetic drift. Evolution 57:1747–1760.

Kirkpatrick, M. 1982. Sexual selection and the evolution of female choice. Evolution 36:1–12.

———. 1985. Evolution of female choice and male parental investment in polygynous species: the demise of the "sexy son." American Naturalist 125:788–810.

———. 1996. Good genes and direct selection in the evolution of mating preferences. Evolution 50:2125–2140.

Kuijper, B., I. Pen, and F. J. Weissing. 2012. A guide to sexual selection theory. Annual Review of Ecology, Evolution, and Systematics 43: 287–311.

Laman, T., and E. Scholes. 2014. Birds of paradise: revealing the world's most extraordinary birds. National Geographic, Washington, DC.

Lande, R. 1976*a*. The maintenance of genetic variability by mutation in a polygenic character with linked loci. Genetical Research 26: 221–235.

———. 1976*b*. Natural selection and random genetic drift in phenotypic evolution. Evolution 30:314–334.

———. 1979. Quantitative genetic analysis of multivariate evolution, applied to brain: body size allometry. Evolution 33:402–416.

———. 1980*a*. The genetic covariance between characters maintained by pleiotropic mutations. Genetics 94:203–215.

———. 1980*b*. Sexual dimorphism, sexual selection, and adaptation in polygenic characters. Evolution 34:292–305.

———. 1981. Models of speciation by sexual selection on polygenic traits. Proceedings of the National Academy of Science of the USA 78:3721–3725.

Lande, R., and S. J. Arnold 1985. Evolution of mating preference and sexual dimorphism. Journal of Theoretical Biology 117:651–664.

LeCroy, M. 1981. The genus *Paradisaea*: display and evolution. American Museum Novitates 2714:1–52.

Maynard Smith, J. 1982. Evolution and the theory of games. Cambridge University Press, Cambridge.

Mead, L. S., and S. J. Arnold. 2004. Quantitative genetic models of sexual selection. Trends in Ecology and Evolution 19:264–271.

Palmer, C. A., A. Picard, R. A. Watts, L. D. Houck, and S. J. Arnold. 2010. Rapid evolution of plethodontid modulating factor (PMF), a hypervariable salamander courtship pheromone, is driven by positive selection. Journal of Molecular Evolution 70:427–440.

Palmer, C. A., R. A. Watts, R. Gregg, M. McCall, L. D. Houck, R. Highton, and S. J. Arnold. 2005. Lineage-specific differences in evolutionary mode in a salamander courtship pheromone. Molecular Biology and Evolution 22:2243–2256.

Palmer, C. A., R. A. Watts, L. D. Houck, A. Picard, and S. J. Arnold. 2007. Evolutionary replacement of components in a salamander pheromone signaling complex: more evidence for phenotypic-molecular decoupling. Evolution 61:202–215.

Pomiankowski, A. 1987. The costs of choice in sexual selection. Journal of Theoretical Biology 128:195–218.

Pomiankowski, A., and Y. Iwasa. 1993. Evolution of multiple sexual preferences by Fisher's runaway process of sexual selection. Proceedings of the Royal Society B: Biological Sciences 253:173–181.

———. 1998. Runaway ornament diversity caused by Fisherian sexual selection. Proceedings of the National Academy of Science of the USA 95:5106–5111.

Pomiankowski, A., Y. Iwasa, and S. Nee. 1991. The evolution of costly mate preferences. I. Fisher and biased mutation. Evolution 45: 1422–1430.

Pruett-Jones, S. G., and M. A. Pruett-Jones. 1990. Sexual selection through female choice in Lawes' parotia, a lek-mating bird of paradise. Evolution 44:486–501.

Ritchie, M. G. 2007. Sexual selection and speciation. Annual Review of Ecology, Evolution, and Systematics 38:79–102.

Scholes, E., III. 2008. Evolution of the courtship phenotype in the bird of paradise genus *Parotia* (Aves: Paradisaeidae): homology, phylogeny, and modularity. Biological Journal of the Linnean Society 94:491–504.

Symonds, M. R. E., and M. A. Elgar. 2008. The evolution of pheromone diversity. Trends in Ecology and Evolution 23:220–228.

Uyeda, J. C., S. J. Arnold, P. A Hohenlohe, and L. S. Mead. 2009. Drift promotes speciation by sexual selection. Evolution 63:583–594.

Uyeda, J. C., T. F. Hansen, S. J. Arnold, and J. Pienaar. 2011. The million-year wait for macroevolutionary bursts. Proceedings of the National Academy of Sciences of the USA 108:15908–15913.

Uyeda, J. C., and L. K. Harmon. 2014. A novel Bayesian method for inferring and interpreting the dynamics of adaptive landscapes from phylogenetic comparative data. Systematic Biology 63:902–918.

van Doorn, G. S., and F. J. Weissing. 2004. The evolution of female preferences for multiple indicators of quality. American Naturalist 164:173–186.

———. 2006. Sexual conflict and the evolution of female preferences for indicators of male quality. American Naturalist 168:742–757.

Wedekind, C. 1994. Mate choice and maternal selection for specific parasite resistances before, during and after fertilization. Philosophical Transactions of the Royal Society B: Biological Sciences 346:303–311.

Wright, S. 1934. An analysis of variability in number of digits in an inbred strain of guinea pigs. Genetics 19:506–536.

Wyatt, T. D. 2014. Pheromones and animal behavior. 2nd ed. Cambridge University Press, Cambridge.

Associate Editor: Locke Rowe
Editor: Susan Kalisz